Effects of Primary Aromatic and Primary Aliphatic Amines on the Formation of Cardanol-Based Benzoxazine Monomers Based on Fourier-transform Infrared and Raman Spectroscopy

Dini Harsanti
Department of Metallurgical and Materials Engineering, Universitas Indonesia

Anne Zulfia Syahrial
Department of Metallurgical and Materials Engineering, Universitas Indonesia

Yudi Nugraha Thaha
Research Center for Metallurgical, National Research and Innovation Agency (BRIN)

Bagus Hayatul Jihad
Research Center for Rocket Technology, National Research and Innovation Agency (BRIN)

他

https://doi.org/10.5109/7402651

出版情報：Evergreen. 12 (4), pp.2223-2235, 2025-12. Interdisciplinary Graduate School of Engineering Sciences, Kyushu University, Japan
バージョン：

Effects of Primary Aromatic and Primary Aliphatic Amines on the Formation of Cardanol-Based Benzoxazine Monomers Based on Fourier-transform Infrared and Raman Spectroscopy

Dini Harsanti[1,2,*], Anne Zulfia Syahrial[1], Yudi Nugraha Thaha[3], Bagus Hayatul Jihad[4], Joddy Arya Laksmono[2]

[1]Department of Metallurgical and Materials Engineering, Universitas Indonesia, Indonesia
[2]Research Center for Polymer Technology, National Research and Innovation Agency (BRIN), Indonesia
[3]Research Center for Metallurgical, National Research and Innovation Agency (BRIN), Indonesia
[4]Research Center for Rocket Technology, National Research and Innovation Agency (BRIN), Indonesia

*Author to whom correspondence should be addressed:
E-mail: dini.harsanti@ui.ac.id

(Received June 10, 2025; Revised August 06, 2025; Accepted December 17, 2025)

Abstract: High-performance benzoxazine monomers are presenting an interesting challenge in polymer science. The demand for natural phenols, such as cardanol is growing due to shrinking petroleum resources and rising concerns about environmental sustainability. This analysis examines the effects of aromatic and aliphatic amines on the formation of cardanol-based benzoxazine monomers. During the analysis, four benzoxazine precursors prepared from cardanol-aniline (C-an), cardanol-furfurylamine (C-fu), cardanol-laurylamine (C-la), and cardanol-stearylamine (C-sa) were separately reacted with paraformaldehyde via a Mannich condensation reaction mechanism. The functional groups and crystallinity degree of the benzoxazine monomers were investigated using nonlinear Gaussian deconvolution of the fourier transform infrared (FTIR) and Raman spectra. The results indicated cardanol-based benzoxazine synthesized with furfurylamine contained a higher number of oxazine rings than that with aniline, laurylamine, and stearylamine. The Raman spectral analysis showed that the double bond in the carbon structure of the furan ring derived from furfurylamine occurred at the Raman shift of 1505 cm^{-1}. Consequently, the double bond in the carbon structure of the benzene ring originated from aniline and occurred at the Raman shift of 1600 cm^{-1}. The benzoxazine monomer synthesized with furfurylamine showed a degree of crystallinity of 54.49%, signifying a higher number of benzoxazine molecules due to the reactivity of the furan rings in the oxazine ring formation process.

Keywords: aliphatic amines; aromatic amines; benzoxazine; cardanol; degree of crystallinity

1. Introduction

Polybenzoxazine is a thermoset polymer with better thermal stability and mechanical properties than other types of thermosets, including epoxy as well as phenolic[1)]. This polymer has unique properties abscent in other traditional thermoset resins, such as a minimal chance of void formation that provides good mechanical properties. Other properties include high char yield for good thermal stability, minimal volumetric shrinkage for strong dimensional stability, and very low water absorption, which improves resistance to environmental factors. Following this discussion, the crosslinked polybenzoxazine shows good electrical properties when compared to others[2)]. The preparation of benzoxazine monomers via a Mannich-like condensation reaction requires phenols, amines, and paraformaldehyde[3)]. These monomers experiencing a ring-opening reaction (ROP) through a thermal mechanism will produce polybenzoxazine without generating other volatile compounds[4)]. Polybenzoxazine applications include hydrophobic coatings, sound insulators, electrical

Cite: D. Harsanti et al., "Effects of Primary Aromatic and Primary Aliphatic Amines on the Formation of Cardanol-Based Benzoxazine Monomers Based on Fourier-transform Infrared and Raman Spectroscopy". Evergreen, 12 (04) 2223-2235 (2025). https://doi.org/10.5109/7402651.

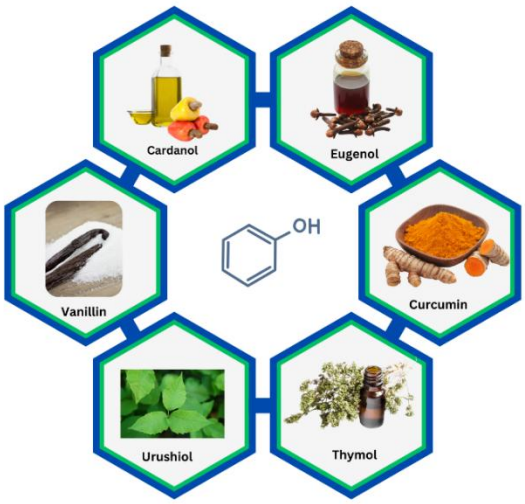

Fig. 1: Various natural phenol compounds

insulators, batteries, oil-water separators, and aerospace components[3].

The source of phenol to synthesize benzoxazine monomers generally uses petroleum-based phenols and each derivative, such as bisphenol-A as well as bisphenol-F[5]. However, the source of phenol from petroleum has limitations, including diminishing petroleum reserves, unstable supply, and fluctuating prices due to the uncertainty of global political conditions. The increasing awareness of environmental sustainability has intensified the search for natural phenols to replace petroleum-based phenols, as the compounds are more readily available. Recently, previous analysis have focused on synthesizing benzoxazine from bio-based phenols (Figure 1), including those from lignin derivatives such as eugenol[6], guaiacol[7], vanillin[8], curcumin[9], cardanol[10], sesamol[10], catechol[11], thymol[12], and urushiol[11]. The challenge in using lignin derivatives such as vanillin and eugenol as reactants to synthesize benzoxazine is the lack of suitable reactive groups[13]. Moreover, the synthesis process of benzoxazine requires phenol groups with unsubstituted ortho-positions. When other functional groups substitute this ortho-position, the benzoxazine ring formation cannot proceed[3]. A phenol compound derived from CNSL (Cashew Nutshell Liquid) known as Cardanol has a phenol functional group in the meta-position, enabling it to have a free ortho-position. Therefore, the free ortho-position on cardanol can serve as a site for the synthesis of the benzoxazine monomer. Long aliphatic side chains substituted at the meta-position give the compound a naturally good hydrophobic behavior, as the side chains reduce the brittleness of the final material[14]. Typically, the composition of CNSL in cashew nuts is 20% - 30% of the total weight of the nuts [9]. Following the discussion, anacardic acid is converted to cardanol through a decarboxylation reaction during CNSL distillation process, producing technical-grade cardanol with a purity of 80-90%[9]. Calo et al. were the first to report the compound use as a phenol source to synthesize benzoxazine monomers[15]. The structure of cardanol includes three reactive groups that enable chemical reactions, including a phenolic hydroxyl group, a carbon double bond in the long alkyl side chain, and aromatic ring[9]. Cardanol as a compound generally has three double bonds in its aliphatic chain. However, these double bonds can vary in molecular weight from 50% monoene, 30% diene, and 20% triene[9].

Previous studies on benzoxazine synthesis used organic solvents including toluene[16], dioxane[17], and chloroform[18], which were harmful to humans when inhaled. Some solvents require a relatively high temperature higher than 100°C to be removed from the benzoxazine monomer, which causes degradation and early polymerization of the benzoxazine compound[19]. Therefore, this study aimed to use an environmentally friendly solvent that is relatively non-hazardous to humans when synthesizing benzoxazine monomers. A suitable solvent for synthesizing benzoxazine monomers should be inert to the oxazine ring formation reaction with a moderate boiling point less than 100°C, and be easily vanished from the final reaction product. The solubility experiment shows that ethyl acetate can completely dissolve the reactants used to form the benzoxazine monomer compared with ethanol. In addition, ethyl acetate is also a type of aprotic dipolar solvent. Aprotic dipolar solvents are widely used in pharmaceutical studies and organic synthesis because of the polarity as well as solubility[20]. The advantage of using aprotic dipolar solvents includes the ability to increase the reaction rate. Due to this reason, ethyl acetate will be used as the solvent in the analysis with an organic solvent composition of approximately 20% by weight of the reaction mixture. This study can be categorized as a green manufacturing method for synthesizing benzoxazine monomers.

Earlier studies had used various primary amines to synthesize benzoxazine monomers, consisting of aliphatic and aromatic amines. Aniline is aromatic amine compound with a phenyl ring attached to the amino group[21]. Ishida et al. first used aniline as a co-reactant of benzoxazine[22], but several studies applied furfurylamine compounds to synthesize benzoxazine monomers. Furfurylamine is a product of the amination reaction of furfural, which is a cyclic organic compound with five carbon atoms. An interesting advantage of using this compound to synthesize benzoxazine monomers is that the interaction between the furan moiety and the oxazine ring during the ROP process improves the thermal properties as well as the density of the crosslinked network[4]. Aliphatic primary amines, such as laurylamine and stearylamine that are obtained from vegetable oils can synthesize benzoxazine monomers. However, the concentration of the oxazine functional group decreased in monomers owing to the long alkyl chain structure[5]. Benzoxazine monomers synthesized from stearylamine as well as laurylamine generally have good hydrophobicity properties and have been used for

surface coating[3].

The changes in the polymers are reflected in the corresponding changes in the spectral band associated with molecular vibrations, as measured by Raman and Fourier transform infrared (FTIR) spectroscopy. Previous studies showed that substituent groups on aromatic rings and side-chain functional groups of amines contributed to the different properties of the final product of cardanol-based benzoxazine monomers[3]. No comprehensive analysis has been conducted on the polymer crystallinity properties of cardanol-based benzoxazine monomers. Therefore, this study is the first to examine the crystallinity of polymers derived from cardanol-based benzoxazine monomers through the introduction of primary amines containing both aromatic as well as aliphatic functional groups. This result investigates in detail the effect of aromatic and aliphatic functional groups of primary amines on cardanol-based benzoxazine monomers as well as the degree of crystallinity of each benzoxazine monomer using FTIR and Raman spectroscopy. The study uses deconvolution with a nonlinear least squares Gaussian function to quantify the degree of crystallinity in benzoxazine monomers based on FTIR and Raman spectra. In this experiment, the synthesis of benzoxazine monomers included using primary amines containing aromatic functional groups, furan rings, and long alkyl chains to investigate the effect on the properties of resulting monomers.

2. Experiment

2.1. Materials

High-purity cardanol (approximately 99%) was obtained from Shanghai Jiangqing International Co, Ltd, in China. Aniline (99%), furfurylamine (Fu, 99%), stearylamine (Sa, 99%), laurylamine (La, 99%), paraformaldehyde (PFA, 95%), sodium hydroxide (NaOH, 99%), ethyl acetate (EA, 99%) and others chemical solvent were obtained from Sigma-Aldrich.

2.2. Measurement

FTIR spectroscopy was used to characterize the synthesized benzoxazine structure. FTIR was a method used for imaging molecular structures based on atomic vibrations. This method showed the precise nature of chemical bonds and molecular structures present in various materials, particularly when analyzing samples related to plastics, polymers, as well as organic components[23]. The band or peak in the FTIR spectra represented the fingerprints of specific molecular structures and chemical bonds[24]. This experiment used a Thermo Fisher Scientific Nicolet iS5 FTIR+NIR spectrometer with an iD7 ATR accessory having 16 additional scans and a resolution of 4 cm^{-1} in absorbance mode. Relating to the process, measurement with FTIR followed the following procedure. A total of 2 g of the benzoxazine monomer was dripped using a dropper on an ATR crystal plate. The sample made close contact with the crystal, allowing the sensor to detect the energy from the absorbed infrared light. Furthermore, the sample contacted the crystal since the penetration depth of the infrared energy was significantly shallow (1-4 micrometers), allowing the sample to absorb the energy to produce an observable spectrum. The spectra were extracted using the OMNIC software, which was included in the FTIR equipment package. The area under the curve of the FTIR spectra was examined using Origin software from OriginLab Corporation.

Raman spectroscopy provided information about the chemical structure, physical condition, quantitative and qualitative amounts of substances in a material as well as identified materials based on the spectral fingerprint patterns. This spectroscopy can completely characterize the benzoxazine monomers structure, sharpening the analysis of the functional groups present in benzoxazine monomers. Raman testing was performed using LabRAM HR Evolution Raman Microscopes HORIBA with a 785 nm laser beam and a 600 g/mm grating. Following the process, the measurement was conducted in the spectral range 200–4000 cm^{-1}.

2.3. Synthesis Method

Cardanol/aniline benzoxazine monomer was prepared from cardanol, paraformaldehyde, and aniline. During the analysis, cardanol (15 grams, 0.05 mol), and paraformaldehyde (3.15 grams, 0.10 mol), were first dissolved in ethyl acetate (4.45 grams, 0.05 mol) in a 50 ml boiling flask until fully dissolved. Aniline (4.65 grams, 0.05 mol) was then given dropwise to the solution. The mixture was refluxed at 90°C for 6 h using a magnetic stirring hot plate. After cooling at ambient temperature, the condensation product was collected into a separatory funnel and washed with 1 M NaOH while adding ethyl acetate solvent until the solution separated into two phases. These phases included the bottom solution comprising NaOH and unreacted or excess components, as well as the solution on top containing benzoxazine monomer. After the separation of the compound, monomer solution was cleaned with distilled water. The benzoxazine monomer was dried with Na_2SO_4 to absorb the remaining water. The solution was then filtered to move the desiccant from monomer. The final step was to remove the ethyl acetate solvent from the benzoxazine monomer solution in a vacuum oven for 24h.

The cardanol/furfurylamine monomer was synthesized with a molar ratio of 15 grams of cardanol (0.05 mol), 3.15 g of paraformaldehyde (0.10 mol), and 4.85 g of furfurylamine (0.05 mol). The cardanol/laurylamine monomer was synthesized with a molar ratio of 15 g of cardanol (0.05 mol), 3.15 g of paraformaldehyde (0.10 mol), and 9.25 g of laurylamine (0.05 mol), and

cardanol/stearylamine monomer was synthesized with a molar ratio of 15 g of cardanol (0.05 mol), 3.15 g of paraformaldehyde (0.10 mol), and 13.5 g of stearylamine (0.05 mol). The products of the reaction were written as C-an signifying cardanol/aniline, C-fu representing cardanol/furfurylamine, C-la for cardanol/laurylamine, and C-sa was cardanol/stearylamine.

3. Results and Discussion

3.1. Molecular Structure Analysis

Figure 2 showed the synthesis route of cardanol-based benzoxazine monomer using primary amines, such as aniline, furfurylamine, laurylamine, and stearylamine, through a Mannich condensation reaction in ethyl acetate as the solvent. The molecular structure of benzoxazine monomers synthesized with aniline had a benzene ring functional group attached to the oxazine ring of the same monomer. The molecular structure of monomers synthesized with furfurylamine had a functional group of furan rings attached to the oxazine ring of the same monomer. Meanwhile, the molecular structure of benzoxazine monomers synthesized with laurylamine and stearylamine had a long aliphatic carbon chain corresponding to the number of carbon atoms.

The volume of reactants that reacted increased proportionally with the same molar ratio because of the more carbon and hydrogen atoms in stearylamine than in laurylamine in cardanol/stearylamine formulation. However, the low reactivity of the reaction caused the product to be more dilute than other amine formulations. The higher dilution of cardanol/stearylamine monomer showed that monomer was more suitable for coating

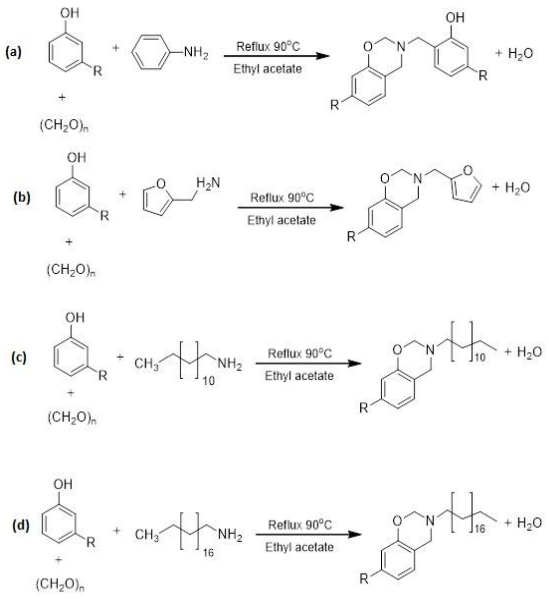

Fig. 2: Benzoxazine monomer synthesis routes: (a) cardanol/aniline, (b) cardanol/furfurylamine, (c) cardanol/laurylamine, and (d) cardanol/stearylamine

applications compared to structural usage. The low reactivity of aliphatic amines led to low crosslinking in the resulting polymer. This occurred because cross-bonding in three-dimensional polymer networks, such as polybenzoxazine, included chemical crosslinking formed by covalent bonds between polymer chains[25]. The benzoxazine monomers produced by aliphatic amines were challenging to crosslink due to the limited number of oxazine ring molecules, which led to polymers with reduced strength and stability. In addition, the pure C-an and C-fu benzoxazine monomers showed higher viscosity than the C-la as well as C-sa benzoxazine monomers in the synthesis process. The obtained yields were 80% C-an, 75% C-fu, 65% C-la, and 50% C-sa monomer.

3.2. FTIR Spectral Analysis

In the context of this study, the FTIR spectrum of C-an monomer was shown in Figure 3a. The absorbance band at wavenumber 3006 cm^{-1} corresponded to the C–H stretching vibration because of olefinic unsaturated aromatic compound from cardanol[26]. The absorbance band at wavenumbers 2922 and 2851 cm^{-1} represented asymmetric as well as symmetric C–H stretching vibrations of the long-chain linear benzoxazine compound[27]. Additionally, the range at 1622 cm^{-1} matched the aryl-substituted C=C stretching vibration of the benzoxazine[18]. The line at 1600 cm^{-1} and 1496 cm^{-1} agreed with the C═C stretching vibration of the benzene ring from the aniline aromatic ring[28]. The band at wavenumber 1577 cm^{-1} matched the C=C aromatic ring stretching vibration in the benzoxazine[29]. Moreover, the range wavenumber 1429 and 1370 cm^{-1} corresponded to the C–H asymmetric and symmetric bending vibration of aliphatic alkyl in the benzoxazine[23]. The band at 1255, 1240, and 1198 cm^{-1} agreed with the C–O stretching oxazine ring vibration [4]. The range at 1143 and 1113 cm^{-1} corresponded to the C–C skeletal stretching vibration of the oxazine ring[30]. In addition, the band at 1031 cm^{-1} matched the C–N stretching vibration of the oxazine ring[31]. The band at wavenumber 989 and 960 cm^{-1} agreed with the C–H out-of-plane bending vibration and trans-C–H out-of-plane bending vibrations in the benzoxazine[18]. Furthermore, the absorbance range at 905, 868, and 798 cm^{-1} corresponded to the C–H 1,3-Disubstitution (meta) absorption in the benzoxazine[23]. The group wavenumber at 750 cm^{-1} was the benzene ring of aniline. The band at 720 cm^{-1} agreed with the C–H rocking vibration of the benzoxazine[30]. The range at wavenumber 692 cm^{-1} corresponded to the C–H bending vibration of aromatic benzene ring[31]. The absorbance band at 627 cm^{-1} was attributed to the ≡C–H benzoxazine bending vibration[30].

The FTIR spectrum of the C-fu monomer was shown in Figure 3(b). The absorbance band appearing at wavenumbers region included the following, 3008 cm^{-1} (C–H stretching vibration)[24], 2923 and 2851 cm^{-1}

Cite: D. Harsanti et al., "Effects of Primary Aromatic and Primary Aliphatic Amines on the Formation of Cardanol-Based Benzoxazine Monomers Based on Fourier-transform Infrared and Raman Spectroscopy". Evergreen, 12 (04) 2223-2235 (2025). https://doi.org/10.5109/7402651.

(asymmetric and symmetric C–H aliphatic stretching vibration)[32]. Other wavenumbers were 1622 cm^{-1} (C=C stretching vibration)[24], 1576 and 1504 cm^{-1} (C=C stretching vibration)[23], 1429 cm^{-1} (asymmetric C–H stretching vibration)[33], 1361 cm^{-1} (symmetric C–H rocking vibration)[34], as well as 1240 cm^{-1} (C–O stretching vibration). Additionally, 1148 and 1109 cm^{-1} (C–C skeletal stretching vibration), 1076 and 1011 cm^{-1} (oxazine ring and ring breathing of the furan ring, which referred to the C–N in phase bonding and symmetric stretching vibrations of the C–C bonding)[35], 993 cm^{-1} (C–H out-of-plane bending vibration)[23], 967 cm^{-1}, and (trans C–H out-of-plane bending vibration). The wavenumber included 913, 885, 865, and 805 cm^{-1} (C–H 1,3-Disubstitution (meta) absorption)[36], 730 cm^{-1} (C–H rocking vibration of the benzoxazine and furan ring)[37], as well as 630 cm^{-1} (≡C–H bending vibration)[30].

The observable difference in the vibrational spectrum between the C-an and C-fu monomers was the existence of band at 1011 cm^{-1} (Figure 3b), showing the presence of the furan ring from furfurylamine. Meanwhile, the band at 1600, 1031, 750, and 692 cm^{-1} (Figure 3a) signified aromatic benzene rings from aniline (stretching vibrations of the C=C–C, C–N, and C–H). The fingerprint region at the band 730 cm^{-1} in C-fu had a higher absorbance intensity. This higher peak intensity was possibly due to the combination of the C–H rocking vibration peak and the furan ring.

During the analysis, the FTIR spectrum of the C-la monomer was shown in Figure 4a. The absorbance band appearing at wavenumbers region included 3007 cm^{-1} (C–H stretching vibration), 2921 and 2851 cm^{-1} (symmetric and asymmetric C–H aliphatic stretching vibration), as well as 1622 cm^{-1} (conjugated C=C of aliphatic alkene of the oxazine ring). Other band comprised 1576 and 1504 cm^{-1} (C=C and C–C bonding stretching vibration of the oxazine ring), 1464 cm^{-1} (C–H bending vibration)[38], 1429 cm^{-1} (asymmetric C–H rocking vibration), 1375 cm^{-1} (symmetric C–H rocking vibration), 1239 cm^{-1} (asymmetric C–O stretching vibration of the oxazine ring), and 1116 cm^{-1} (O–C–O skeletal stretching vibration)[28]. Additionally, 987 and 963 cm^{-1} (C–H out-of-plane bending vibration and trans-C–H out-of-plane bending vibration), 909, 887, 867, and 802 cm^{-1} (C−H 1,3-Disubstitution (meta) absorption), 720 cm^{-1} (C–H rocking vibration of the benzoxazine)[24], and 630 cm^{-1} (≡C−H bending vibration)[30].

The FTIR spectrum of the C-sa monomer was shown in Figure 4b. The absorbance band appearing at wavenumbers region included 3007 cm^{-1} (C–H stretching vibration), 2919 and 2850 cm^{-1} (asymmetric and symmetric C–H aliphatic stretching vibration), 1623 cm^{-1} (C=C stretching vibration), 1577 and 1506 cm^{-1} (C=C stretching vibrations), 1463 cm^{-1} (C–H bending vibration)[24] as well as 1429 cm^{-1} (asymmetric C–H rocking vibration), 1375 cm^{-1} (symmetric C–H rocking vibration), 1240 cm^{-1} (asymmetric C–O stretching vibration). Other wavenumbers region comprised 1118 cm^{-1} (C–C symmetric stretching vibration), 987 and 963 cm^{-1} (C–H out-of-plane bending vibration and trans-C–H out-of-plane bending vibration), 909, 887, 867, and 803 cm^{-1} (C–H 1,3-Disubstitution (meta) absorption), 720 cm^{-1} (C–H rocking vibration)[24], as well as 634 cm^{-1} (≡C–H bending vibration)[30]. The observable difference between the C-la monomer and the C-sa monomer was the absorbance intensity value of the band, where the benzoxazine functional groups in C-sa were lower in absorbance intensity compared to C-la. This showed that more benzoxazine functional groups were formed in formulations with short-chain aliphatic primary amines such as laurylamine compared to formulations of aliphatic primary amines having longer chains including stearylamine. Following the discussion, laurylamine was more reactive than stearylamine in the analysis. The band

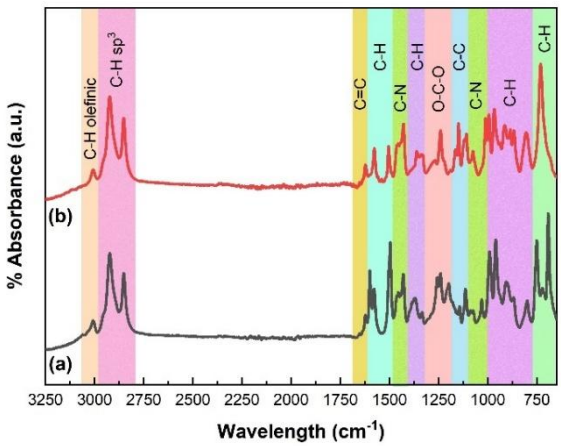

Fig. 3: FTIR spectra of (a) cardanol/aniline benzoxazine and (b) cardanol/furfurylamine benzoxazine

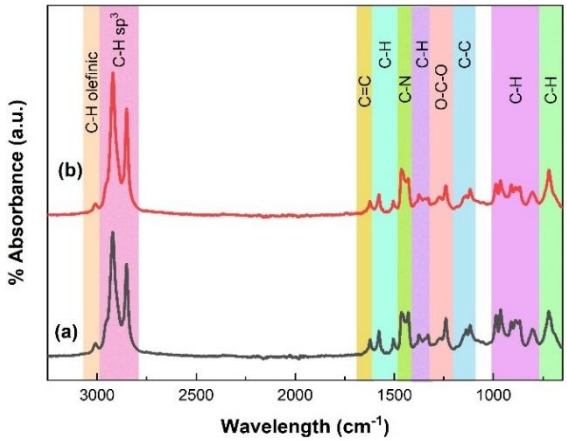

Fig. 4: FTIR spectra of (a) cardanol/laurylamine benzoxazine and (b) cardanol/stearylamine benzoxazine

Cite: D. Harsanti et al., "Effects of Primary Aromatic and Primary Aliphatic Amines on the Formation of Cardanol-Based Benzoxazine Monomers Based on Fourier-transform Infrared and Raman Spectroscopy". Evergreen, 12 (04) 2223-2235 (2025). https://doi.org/10.5109/7402651.

at 1329 and 1137 cm^{-1} were not formed in the C-sa monomer due to a lack of stearylamine reactivity. The FTIR spectra of benzoxazine monomers synthesized with aromatic primary amines (Figure 3) and those synthesized with aliphatic primary amines (Figure 4) showed a clear difference in the number of peaks produced. Specifically, benzoxazine monomers synthesized with aromatic primary amines signified more peak than those produced with aliphatic primary amines. The intensity of the absorption peak from the functional groups was higher in benzoxazine monomers synthesized with aromatic primary amines compared to those produced with aliphatic primary amines. This outcome showed that a greater number of molecules were produced when using aromatic primary amines rather than aliphatic primary amines. The C-N bonds formation in the oxazine ring was more prevalent in benzoxazine incorporating aromatic primary amines than in those that use aliphatic primary amines. Moreover, no C–N peak was detected in the wavelength range of approximately 1000 cm^{-1} in the benzoxazine with aliphatic primary amines. The absence of the peak showed a low formation of oxazine rings when benzoxazine reacted with aliphatic primary amines, which prevented monomers C-la and C-sa from polymerizing effectively.

3.3. Raman Spectral Analysis

The Raman spectrum of C-an monomer was shown in Figure 5a. The peak at Raman shifts 3015 cm^{-1} corresponded to the =C–H stretching vibration due to olefinic unsaturated aromatic compound. The point at 2922 and 2851 cm^{-1} represented asymmetric and symmetric C–H stretching vibrations of the long-chain linear benzoxazine compound. Additionally, the peak at 1651 cm^{-1} matched the C=C stretching vibration of the oxazine ring. The point at 1600 cm^{-1} corresponded to the C═C stretching vibration of the benzene ring from the aniline aromatic ring. Moreover, the band at 1437 cm^{-1} agreed with the CH_2 and CH_3 asymmetric stretching vibration of aromatic ring in the oxazine. The Raman peak at 1031 cm^{-1} was related to the C–H in-plane deformation of aromatic ring of aniline. The point at 1000 cm^{-1} matched the C–C stretching vibration of aromatic ring chain vibration of aniline. The peak at 739 cm^{-1} corresponded to the C–C skeletal stretching vibration of the oxazine ring.

The Raman spectrum of C-fu monomer was shown in Figure 5b. The peak at Raman shifts 3012 cm^{-1} corresponded to the =C–H stretching vibration due to olefinic unsaturated aromatic compound. The point at 2917 and 2849 cm^{-1} represented asymmetric and symmetric C–H stretching vibrations of the long-chain linear benzoxazine compound. In addition, the peak at 1656 cm^{-1} matched the C=C stretching vibration of the oxazine ring. The point at 1505 cm^{-1} agreed with the C═C stretching vibration of the furan ring from the furfurylamine aromatic ring. The peak at 1440 cm^{-1} corresponded to the CH_2 and

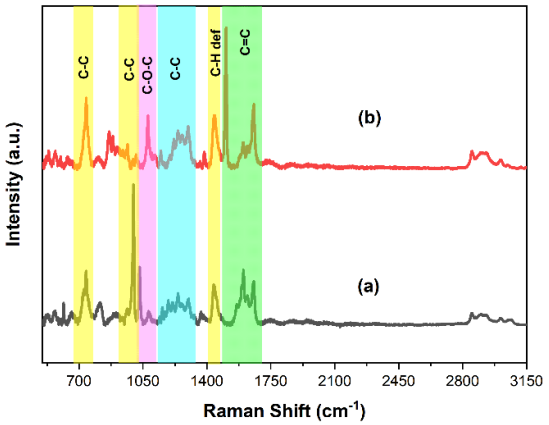

Fig. 5: Raman spectra of (a) cardanol/aniline benzoxazine and (b) cardanol/furfurylamine benzoxazine

CH_3 asymmetric stretching vibration of aromatic ring in the oxazine. Moreover, the point at 1077 cm^{-1} was related to the O–C–O asymmetric from the oxazine ring, and 739 cm^{-1} corresponding to the C–C skeletal stretching vibration of the oxazine ring. The fundamental difference observed in the Raman spectra of C-an and C-fu was the presence of functional groups from each interacting amine was distinguished, such as the benzene ring functional group in C-an at Raman peak 1600 cm^{-1} and the furan ring functional group in C-fu at Raman peak 1505 cm^{-1}, respectively. The advantage of using Raman analysis was its ability to strongly detect functional groups with double and triple bonds more effectively than FTIR.

Figure 6a showed the Raman spectrum of C-la monomer during the analysis. The peak at Raman shifts 3011 cm^{-1} corresponded to the =C–H stretching vibration because of the olefinic unsaturated aromatic compound. The peak at 2922 and 2852 cm^{-1} indicated asymmetric and symmetric C–H stretching vibrations of the long-chain linear benzoxazine compound. Additionally, the point at 1656 cm^{-1} matched the C=C stretching vibration of the oxazine ring. The peak at 1438 cm^{-1} corresponded to the CH_2 and CH_3 asymmetric stretching vibration of aromatic ring in the oxazine. Furthermore, the Raman point at 1298 cm^{-1} was related to the C–C aliphatic chain vibration. The peak at 1077 cm^{-1} agreed with the O–C–O asymmetric from the oxazine ring, and Raman shift 739 cm^{-1} corresponded to the C–C skeletal stretching vibration of the oxazine ring.

The Raman spectrum of C-sa monomer in the analysis was shown in Figure 6b. The peak at Raman shifts 3009 cm^{-1} corresponded to the =C–H stretching vibration because of olefinic unsaturated aromatic compound. Additionally, the point at 2929 and 2849 cm^{-1} showed asymmetric and symmetric C–H stretching vibrations of the long-chain linear benzoxazine compound. The peak at 1658 cm^{-1} matched the C=C stretching vibration of the oxazine ring. The bans at 1436 cm^{-1} corresponded to the CH_2 and CH_3 asymmetric stretching vibration of aromatic ring in the oxazine. Moreover, the Raman peak at 1298 cm^{-1} was

Cite: D. Harsanti et al., "Effects of Primary Aromatic and Primary Aliphatic Amines on the Formation of Cardanol-Based Benzoxazine Monomers Based on Fourier-transform Infrared and Raman Spectroscopy". Evergreen, 12 (04) 2223-2235 (2025). https://doi.org/10.5109/7402651.

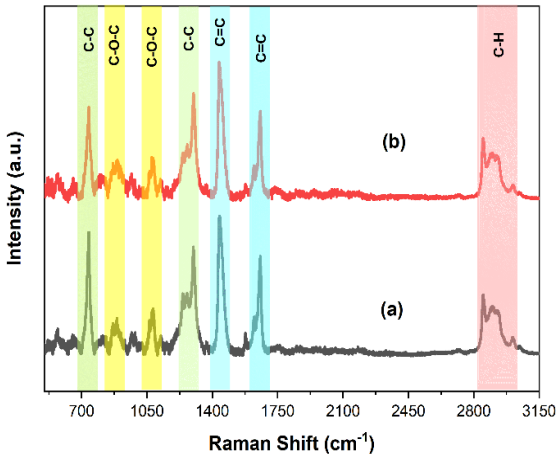

Fig. 6: Raman spectra of (a) cardanol/laurylamine benzoxazine and (b) cardanol/stearylamine benzoxazine

related to the C–C aliphatic chain vibration. The point at 1077 cm^{-1} agreed with the O–C–O asymmetric from the oxazine ring, and 739 cm^{-1} corresponded to the C–C skeletal stretching vibration of the oxazine ring. Following this discussion, the fundamental difference observed in the Raman spectra of C-la and C-sa was the presence of functional groups specific to each amine, particularly the aliphatic functional groups found in both precursors. Due to the shorter aliphatic chain in laurylamine compared to stearylamine, there was a peak shift toward a lower Raman Shift from 1300 to 1298 cm^{-1} in the C-la monomer.

3.4. The Degree of Crystallinity Analysis of Raman Spectra

Raman scattering provided essential information about chemical bonds and structures, intermolecular interactions in a material, crystallinity, molecular stress/strain, as well as the crystalline and amorphous phases of a material[39]. Raman scattering occurred because of molecular vibrations that change the polarizability of the electron cloud around the molecule. This phenomenon originated from the incident light and the molecule interaction, where the energy from the light caused the molecule to vibrate. In Raman scattering, the largest changes in polarizability and the most intense scattering were generally initiated from symmetric molecular vibrations. These vibrations included the stretching or bending of bonds in a molecule, leading to a change in the distribution of electrons and polarizability of the molecule. The largest dipole changes and the most intense absorptions were caused by asymmetric molecular vibrations which were different from FTIR spectroscopy. Asymmetric vibrations caused a greater change in the molecule dipole moment such as those including the rotation of a functional group, leading to more intense absorption in FTIR spectroscopy.

The strength of a bond was directly related to frequency of the bond in Raman spectroscopy. Specifically, stronger bonds were associated with higher frequencies, as weaker bonds were connected to lower frequencies. The mass of the atoms included in the bond also played a role, as light atoms tended to produce higher vibration frequencies than heavy atoms. FTIR and Raman spectroscopy methods were applied to evaluate the crystallinity degree of a polymer[40]. Moreover, the composition of the crystalline phase in polymers determined many macroscopic properties, such as mechanical properties, which increased with increasing crystallinity[41]. The initial step in analyzing the crystallinity degree was to identify the absorption band generated by the amorphous and crystalline phases of the polymer chain[41]. The crystallinity degree was measured as the crystalline phase intensity ratio to the total integrated intensity, as shown in Eq. 1.

$$Dc = \frac{Ic}{(Ic+Ia)} \times 100\% \quad (1)$$

DC was the degree of crystallinity, I_c represented the crystalline phase intensity, and I_a signified the amorphous phase intensity.

In previous analysis, Raman spectroscopy was used to evaluate the local crystallinity on material surfaces. The crystallinity degree, as shown by the Raman shift of 1651 cm^{-1}, signified the strongest statistical correlation with the crystallinity degree measured from density measurements[42]. The peak at the Raman shift of ~1440 cm^{-1}, associated with $>CH_2$ deformation, corresponded to the polymer amorphous phase. The polymer amorphous phase had a higher disorder and randomness degree in its molecular structure, leading to a greater number of CH_2 deformation modes that contributed to the Raman signal. Therefore, the peak observed at Raman shift of 1436, 1438, and 1441 cm^{-1} were characteristic of the amorphous phase of the C-sa, C-an, and C-la, as well as C-fu benzoxazine monomer, respectively.

The degree of crystallinity of C-an monomer from the Raman spectra were measured applying the crystalline

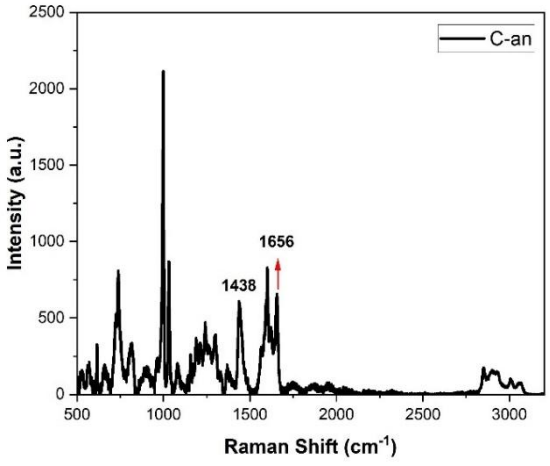

Fig. 7: Raman spectra of cardanol/aniline benzoxazine monomer

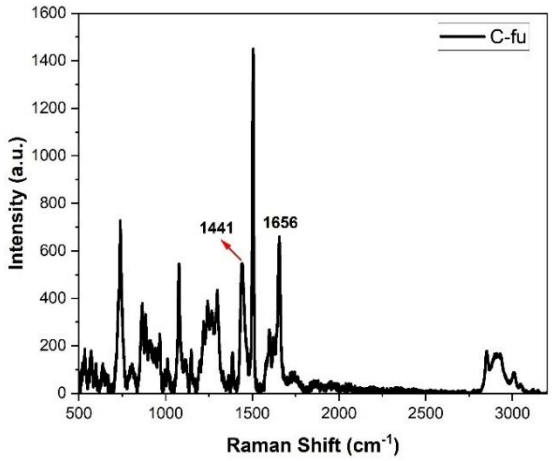

Fig. 8: Raman spectra of cardanol/furfurylamine benzoxazine monomer

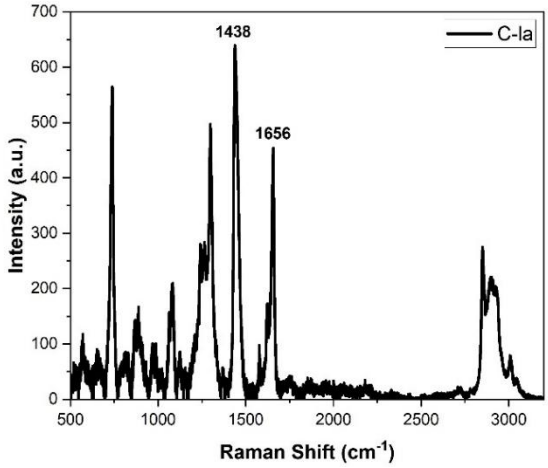

Fig. 9: Raman spectra of cardanol/laurylamine benzoxazine monomer

peak intensity at Raman shift 1656 cm^{-1} with a value of 664.26 and the amorphous peak at Raman shift 1438 cm^{-1} with a value of 617.57 (Figure 7). Using Eq. 1, the crystallinity degree of the benzoxazine C-an monomer was determined to be 51.83%.

The degree of crystallinity of C-fu monomer from the Raman spectrum was measured applying the crystalline peak intensity at Raman shift 1656 cm^{-1} with a value of 664.63 and amorphous point at 1441 cm^{-1} having a value of 551.44, respectively (Figure 8). The crystallinity degree of the benzoxazine C-fu monomer was determined to be 54.49%.

The degree of crystallinity of C-la monomer from the Raman spectrum was measured applying the crystalline peak intensity at Raman shift 1656 cm^{-1} with a value of 455.57 and the amorphous point at 1438 cm^{-1} having a value of 641.37 (Figure 9). In addition, the crystallinity degree of the benzoxazine C-fu monomer was determined to be 41.53%.

The degree of crystallinity of C-sa monomer from the Raman spectrum was measured applying the crystalline

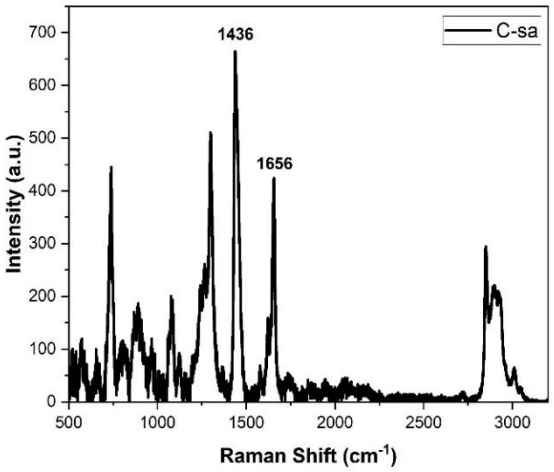

Fig. 10: Raman spectra of cardanol/stearylamine benzoxazine monomer

peak intensity at Raman shift 1656 cm^{-1} with a value of 425.93 and the amorphous point at 1438 cm^{-1} having a value of 667.66 (Figure 10). Additionally, the crystallinity degree of the benzoxazine C-sa monomer was determined to be 38.95%.

Further analysis of the Raman spectral intensity data for all benzoxazine monomers at the ~1440 cm^{-1} band showed that the C-fu monomer signified a shift toward the highest wavenumber at 1441 cm^{-1} (Figure 8). This showed that the C-fu benzoxazine monomer had a lower amorphous phase than other benzoxazine monomer. The shift observed in the C-fu benzoxazine monomer was consistent with its molecular structure, which contained fewer aliphatic C-H chains than other monomers. Consequently, the C-sa monomer signified a shift toward the lowest wavenumber in the 1436 cm^{-1} band (Figure 10). This result confirmed that the C-sa monomer had a higher amorphous phase than other benzoxazine monomers. The shift observed in the C-sa monomer was consistent with its molecular structure, which contained more aliphatic C-H chains than the C-la monomer. Following this discussion, benzoxazine monomers were more effectively synthesized using aromatic primary amines than aliphatic primary amines. This was due to the inherent properties of aromatic primary amines that facilitated the formation of benzoxazine monomers. The use of furfurylamine as primary amine for the synthesis of benzoxazine produced better results than aniline. The reason for this achievement was the furan ring in furfurylamine, which provided additional reactivity and stability to the benzoxazine monomer.

The difference in the Raman shifts for band in the range of ~3010, ~2900, and ~2800 cm^{-1} was a significant indicator of the structural variation in benzoxazine monomers. Specifically, the Raman intensity of benzoxazine monomers synthesized with aromatic amines (C-an and C-fu) was significantly lower compared to monomers produced with aliphatic amines (C-la and C-sa). The difference in intensity was directly correlated with the

conformational state of the C–H bonds in the benzoxazine monomers, showing that monomers synthesized with aromatic amines had higher crystalline phase content compared to those produced through aliphatic amines.

3.5. The Degree of Crystallinity Analysis of FTIR Spectra Deconvolution

The peak of the infrared wavelength spectrum absorption of the polymers was affected by crystallinity[43]. FTIR spectroscopy made it possible to identify changes in the crystalline orientation and amorphous phases during the polymer crystallization process as well as to distinguish crystal forms. The method was also allowed to observe changes in polymer structures and kinetics, detect conformational transformations in polymer chains, and characterize polymer molecular structures[44]. The initial step in analyzing the degree of crystallinity was to identify the absorption band generated by the amorphous and crystalline phases of the polymer chain[41]. The crystallinity degree was measured as the crystalline phase ratio area to the total integrated area, as shown in Eq. 2.

$$Dc = \frac{Ac}{(Ac+Aa)} \times 100\% \qquad (2)$$

DC was the crystallinity degree, A_c represented the crystalline phase area, and A_a signified the amorphous phase area. The nonlinear Gaussian function method was used to find the area under the FTIR spectrum curve to calculate the degree of crystallinity of the benzoxazine monomer based on the spectrum[45].

In the FTIR spectra of the benzoxazine monomer that were shown in Figure 3 and 4, the absorption band at a wavelength of 720 cm^{-1} typically comprised both the crystalline as well as amorphous phases of the polymer. During this study, the fingerprint region of 780 cm^{-1} to 640 cm^{-1} was used to analyze the degree of crystallinity of the benzoxazine monomers. The deconvolution steps of FTIR spectra obeyed the procedure as follows. (1) Corrected the baseline curve of FTIR spectra in the fingerprint region by selecting 780 cm^{-1} and 640 cm^{-1} as correction points with Origin software. (2) The baseline-corrected FTIR spectra curve was then analyzed by running the nonlinear Gaussian fitting method with Origin software. Figure 11 and Table 1 showed the deconvolution result with a Gaussian function calculated from the FTIR spectra of C-an monomer. Four peaks existed at 780 cm^{-1} to 640 cm^{-1}, with band at 751, 722, 692, and 683 cm^{-1}.

However, only the band at 722 cm^{-1} showed the crystalline phase during the process. The degree of crystallinity of C-an monomer was approximately 22.73% using Eq. 1.

Table 1: The area under the curve of C-an monomer

Peak (cm^{-1})	A	A_{ratio}(%)	Adj. R^2
751	3.12 ± 0.05	32.99	0.99692
722	2.15 ± 0.10	22.73	
692	2.12 ± 0.07	22.39	
683	2.07 ± 0.17	21.89	

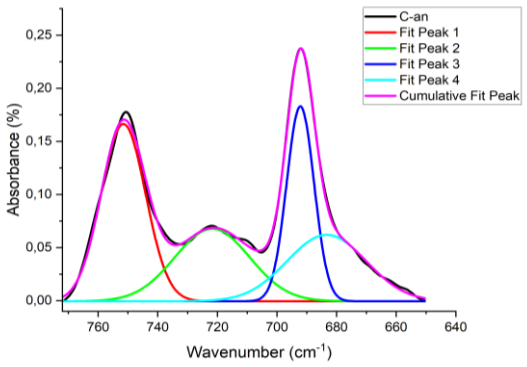

Fig. 11: Gaussian fitting curve for C-an monomer

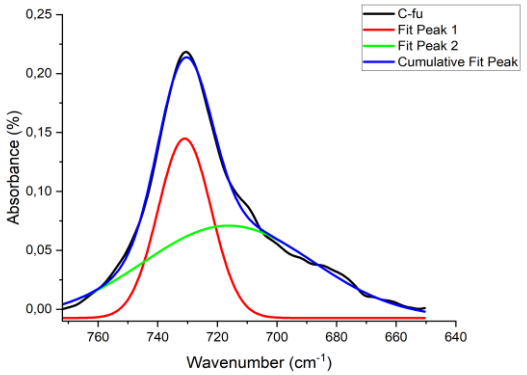

Fig. 12: Gaussian fitting curve for C-fu monomer

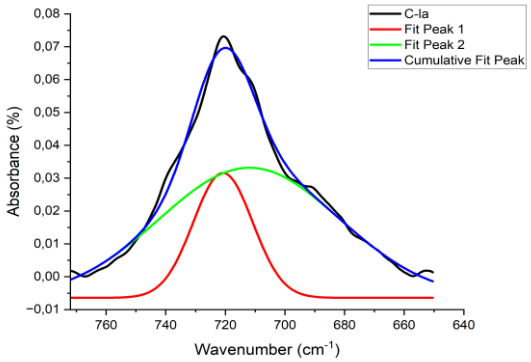

Fig. 13: Gaussian fitting curve for C-la monomer

Table 2: The area under the curve of C-fu monomer

Peak (cm^{-1})	A	A_{ratio}(%)	Adj. R^2
687	1.26 ± 0.05	15.59	0.99995
727	5.42 ± 0.04	65.01	
731	1.58 ± 0.05	19.40	

Table 3: The area under the curve of C-la monomer

Peak (cm^{-1})	A	A_{ratio}(%)	Adj. R^2
720	0.95 ± 0.04	24.01	0.9922
712	3.00 ± 0.16	75.99	

Figure 12 and Table 2 showed the nonlinear Gaussian deconvolution results of the FTIR spectra of the C-fu monomer. Three peaks appeared at 780 to 640 cm^{-1}, with band at 727 cm^{-1} signifying the crystalline region and 687 and 731 cm-1 showing the amorphous region. Moreover, the degree of crystallinity of C-fu monomer was approximately 65.01%.

Figure 13 and Table 3 showed the nonlinear Gaussian deconvolution results of the FTIR spectra of C-la monomer. Two peaks appeared at 780 cm^{-1} to 640 cm^{-1}, with 712 cm^{-1} signifying the amorphous phase and 720 cm^{-1} showing the crystalline phase. In addition, the degree of crystallinity of the C-la monomer was approximately 24.01%.

Figure 14 and Table 4 showed the nonlinear Gaussian deconvolution results of the FTIR spectra of C-sa monomer. Two peak band appeared at 780 cm-1 to 640 cm^{-1}, with 720 cm^{-1} and 714 cm^{-1} representing the crystalline and amorphous phases. Additionally, the crystallinity degree of the C-sa monomer was approximately 22.58%.

Cardanol-based benzoxazine monomers synthesized with aniline, furfurylamine, laurylamine, and stearylamine had absorbance peak areas of approximately 9.46, 8.99, 3.95, as well as 3.71 from the FT-IR spectra analysis using the deconvolution nonlinear Gaussian function method. These areas correlate with the number of functional groups in monomer. Benzoxazine monomers synthesized from aromatic amines have more benzoxazine functional groups and a higher degree of crystallinity. The slightly larger area under the curve for C-an compared to C-fu was due to the additional benzene functional groups in the C-an monomer in the 1600 cm^{-1} and 751 cm^{-1} region. The degree of crystallinity ratio shows that the C-fu monomer was more crystalline than the C-an monomer. The higher degree of crystallinity of C-fu was confirmed in monomer heating experiment, where the C-fu monomer polymerized faster at lower temperatures than the C-an monomer. The results of FTIR analysis conclude that furfurylamine was the best primary amine for synthesizing cardanol-based benzoxazine monomers compared with the other amines.

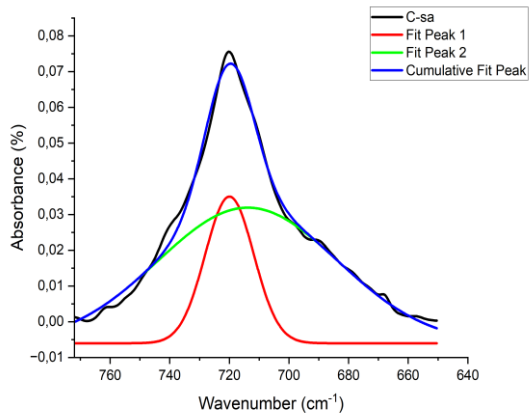

Fig. 14: Gaussian fitting curve for C-sa monomer

Table 4: The area under the curve of C-sa monomer

Peak (cm^{-1})	A	A_{ratio}(%)	Adj. R^2
720	0.83 ± 0.02	22.58	0.99326
714	2.87 ± 0.14	77.42	

4. Conclusions

In conclusion, this study successfully synthesized cardanol-based benzoxazine monomer using a green manufacturing method and an environmentally friendly solvent. The result produced the benzoxazine monomer from cardanol, paraformaldehyde, and four primary amines, namely aniline, furfurylamine, laurylamine, and stearylamine. FTIR spectroscopy analysis showed that benzoxazine monomers synthesized with aromatic primary amines had a higher content of benzoxazine functional groups. In particular, the benzoxazine monomer produced with aniline showed the highest value, signifying higher absorption of infrared waves by the benzoxazine functional groups in the synthesized compounds. Besides the analysis of the functional groups of the benzoxazine monomers, the degree of crystallinity of these monomers was also required because as the degree of crystallinity became higher, the mechanical and thermal properties of the benzoxazine monomer improved. Calculations of crystallinity using FTIR and Raman spectral analysis showed significant differences. The crystallinity values calculated directly from the Raman intensity were higher than those obtained by FTIR spectral deconvolution. Raman spectroscopy provides the most accurate calculation of the degree of crystallinity of cardanol-based benzoxazine monomers because the spectrum has good spatial resolution, thus enabling in-situ crystallinity analysis of monomers with a very small surface area. However, both methods showed the same trend for each benzoxazine monomer, where the compound synthesized with aromatic amines had higher crystallinity degree values than monomers produced through aliphatic amines. Through analysis using Raman spectroscopy and the Gaussian fitting method of FTIR spectroscopy, the study found that the benzoxazine monomer with furfurylamine showed a higher degree of crystallinity than the other monomers. This high value was attributed to furan rings, which were more reactive during the oxazine ring formation.

A limitation of this study was that the degree of crystallinity ratio was not validated using other methods. Recommendations for further studies included characterization by monomer density measurement, GPC, NMR, XRD, and DSC to validate the degree of crystallinity of cardanol-based benzoxazine monomer related to benzoxazine functional groups. Further studies should compare the FTIR and Raman spectra of these four

Cite: D. Harsanti et al., "Effects of Primary Aromatic and Primary Aliphatic Amines on the Formation of Cardanol-Based Benzoxazine Monomers Based on Fourier-transform Infrared and Raman Spectroscopy". Evergreen, 12 (04) 2223-2235 (2025). https://doi.org/10.5109/7402651.

monomers with varying temperature increased to determine conformational changes in the molecular structure of cardanol-based benzoxazine monomers. Additionally, measurements at different temperatures could be used to construct phase diagrams for each cardanol-based benzoxazine monomer.

Acknowledgements

The authors are grateful to Department of Metallurgical and Materials Engineering, Faculty of Engineering, Universitas Indonesia (UI), management of the Study Center for Polymer Technology, National Study and Innovation Agency (BRIN) for the study funding support, and ILRC Laboratory Universitas Indonesia for the technical support.

References

1) S.P. Asrafali, T. Periyasamy, C.J. Raorane, R. Vanaraj, V. Raj, and S.C. Kim, "Development of hybrid titania/polybenzoxazine composite for enhance thermomechanical, flame retardancy and dielectric properties," Sustainability (Switzerland), 15 (2) (2023). doi:10.3390/su15021639.
2) I. Machado, C. Shaer, K. Hurdle, V. Calado, and H. Ishida, "Towards the development of green flame retardancy by polybenzoxazines," Prog Polym Sci, 121 (2021). doi:10.1016/j.progpolymsci.2021.101435.
3) A. Adjaoud, L. Puchot, C.E. Federico, R. Das, and P. Verge, "Lignin-based benzoxazines: a tunable key-precursor for the design of hydrophobic coatings, fire resistant materials and catalyst-free vitrimers," Chemical Engineering Journal, 453 (2023). doi:10.1016/j.cej.2022.139895.
4) F. Li, W. Zhang, and J. Wang, "High-tg bio-based polybenzoxazine derived from renewable anethole and furfurylamine," Eur Polym J, 199 (2023). doi:10.1016/j.eurpolymj.2023.112466.
5) Y. Bi, L. Zu, Z. Zhang, L. Zhang, B. Zhao, S. Cong, T. Lan, S. Dong, Y. Wang, and J. Xu, "Multifunctional biobased benzoxazines: synthesis, copolymerization, and thermal stability studies," ACS Appl Polym Mater, 6 (7) 4282–4289 (2024). doi:10.1021/acsapm.4c00404.
6) P. Thirukumaran, A. Shakilaparveen, and M. Sarojadevi, "Eugenol-Based Polybenzoxazines," in: Advanced and Emerging Polybenzoxazine Science and Technology, Elsevier Inc., 2017: pp. 523–531. doi:10.1016/B978-0-12-804170-3.00027-5.
7) R. Yang, M. Han, B. Hao, and K. Zhang, "Biobased high-performance tri-furan functional bis-benzoxazine resin derived from renewable guaiacol, furfural and furfurylamine," Eur Polym J, 131 (2020). doi:10.1016/j.eurpolymj.2020.109706.
8) M. Derradji, K. Khiari, O. Mehelli, S. Abdous, B. Amri, R. Belgacemi, N. Ramdani, A. Zegaoui, and W. Liu, "Green composites from vanillin-based benzoxazine and silane surface modified chopped carbon fibers," Polymers from Renewable Resources, 14 (1) (2023). doi:10.1177/20412479221147052.
9) T. Periyasamy, S.P. Asrafali, and S.C. Kim, "Bio-based polybenzoxazine–cellulose grafted films: material fabrication and properties," Polymers (Basel), 15 (4) (2023). doi:10.3390/polym15040849.
10) C. Zhang, J. Xue, X. Yang, Y. Ke, R. Ou, Y. Wang, S.A. Madbouly, and Q. Wang, "From plant phenols to novel bio-based polymers," Prog Polym Sci, 125 (2022). doi:10.1016/j.progpolymsci.2021.101473.
11) I. Machado, I. Hsieh, E. Rachita, M.L. Salum, D. Iguchi, N. Pogharian, A. Pellot, P. Froimowicz, V. Calado, and H. Ishida, "A truly bio-based benzoxazine derived from three natural reactants obtained under environmentally friendly conditions and its polymer properties," Green Chemistry, 23 (11) (2021). doi:10.1039/d1gc00951f.
12) S. Khan, S. Masood, A. Ghosal, M. Azam, M. Alam, F. Zafar, Q.M.R. Haq, and N. Nishat, "Mechanically robust and antibacterial coatings constructed from cardanol-aliphatic amine based metal-coordinated nanostructured framework," Prog Org Coat, 188 (2024). doi:10.1016/j.porgcoat.2024.108244.
13) H. Srinivasan, H. Arumugam, S. Rimdusit, and A. Muthukaruppan, "Bio-thymol containing new high-performance thymolphthalein based polybenzoxazine: thermal, superhydrophobic and dielectric properties," Colloids Surf A Physicochem Eng Asp, 675 (2023). doi:10.1016/j.colsurfa.2023.131947.
14) A. Trejo-Machin, A. Adjaoud, L. Puchot, R. Dieden, and P. Verge, "Elucidating the thermal and polymerization behaviours of benzoxazines from lignin derivatives," Eur Polym J, 124 (2020). doi:10.1016/j.eurpolymj.2019.109468.
15) H. Arumugam, B. Krishnasamy, G. Perumal, A.D. A, M.I. Abdul Aleem, and A. Muthukaruppan, "Bio-composites of rice husk and saw dust reinforced bio-benzoxazine/epoxy hybridized matrices: thermal, mechanical, electrical resistance and acoustic absorption properties," Constr Build Mater, 312 (2021). doi:10.1016/j.conbuildmat.2021.125381.
16) E. Calò, A. Maffezzoli, G. Mele, F. Martina, S.E. Mazzetto, A. Tarzia, and C. Stifani, "Synthesis of a novel cardanol-based benzoxazine monomer and environmentally sustainable production of polymers and bio-composites," Green Chemistry, 9 (7) 754–75 (2007). doi:10.1039/b617180j.
17) Y. Xing, X. He, R. Yang, K. Zhang, and S. Yang, "Design of high-performance polybenzoxazines with tunable extended networks based on resveratrol and

allyl functional benzoxazine," Polymers (Basel), 12 (12) 1–10 (2020). doi:10.3390/polym12122794.
18) H.A. Klfout, A.M. Asiri, K.A. Alamry, and M.A. Hussein, "Recent advances in bio-based polybenzoxazines as an interesting adhesive coating," RSC Adv, 13 (29) 19817–19835 (2023). doi:10.1039/d3ra03514j.
19) R. Ganfoud, N. Guigo, L. Puchot, P. Verge, and N. Sbirrazzuoli, "Investigation on the role of the alkyl side chain of cardanol on benzoxazine polymerization and polymer properties," Eur Polym J, 119 (2019). doi:10.1016/j.eurpolymj.2019.07.026.
20) W. Li, and W. Jiang, "Methods for preparing benzoxazines using aqueous solvent," United States Patent, (2012).
21) E.. Buncel, and R.A.. Stairs, "Solvent effects in chemistry," Wiley, 2016.
22) M. Anjalin, N. Kanagathara, and A.R. Baby Suganthi, "A brief review on aniline and its derivatives," in: Mater Today Proc, Elsevier Ltd, 2020: pp. 4751–4755. doi:10.1016/j.matpr.2020.08.358.
23) H. Ishida, and Y. Rodriguez, "Curing kinetics of a new benzoxazine-based phenolic resin by differential scanning calorimetry," 1995.
24) A.B.D. Nandiyanto, R. Oktiani, and R. Ragadhita, "How to read and interpret ftir spectroscope of organic material," Indonesian Journal of Science and Technology, 4 (1) 97–118 (2019). doi:10.17509/ijost.v4i1.15806.
25) A.B.D. Nandiyanto, R. Ragadhita, and M. Fiandini, "Interpretation of fourier transform infrared spectra (ftir): a practical approach in the polymer/plastic thermal decomposition," Indonesian Journal of Science and Technology, 8 (1) 113–126 (2023). doi:10.17509/ijost.v8i1.53297.
26) Z. Xu, Y. Takahashi, and A. Takada, "Elastic modulus of the gel made from interpenetrating polymer networks in phase separated state," Evergreen, 1 (1) 1–5 (2014). doi:10.5109/1440968.
27) P.P. Chiplunkar, and A.P. Pratap, "Utilization of sunflower acid oil for synthesis of alkyd resin," Prog Org Coat, 93 61–67 (2016). doi:10.1016/j.porgcoat.2016.01.002.
28) S. Devaraju, K. Krishnadevi, S. Sriharshitha, and M. Alagar, "Design and development of environmentally friendly polybenzoxazine–silica hybrid from renewable bio-resource," J Polym Environ, 27 (1) 141–147 (2019). doi:10.1007/s10924-018-1327-z.
29) R. Lestari, D. Wahyuningsih, and I. Kartini, "High Quantum Yield Nitrogen-Carbon Dots (N-CDs) from Plastic Waste," 2023.
30) L.R.V. Kotzebue, F.W.M. Ribeiro, V.G. Sombra, J.P.A. Feitosa, G. Mele, S.E. Mazzetto, and D. Lomonaco, "Spectral and thermal studies on the synthesis and catalyzed oligomerization of novel cardanol-based benzoxazines," Polymer (Guildf), 92 189–200 (2016). doi:10.1016/j.polymer.2016.04.005.
31) D. Lin-Vien, N.B. Colthup, W.G. Fateley, and J.G. Grasselli, "Alkanes," in: The Handbook of Infrared and Raman Characteristic Frequencies of Organic Molecules, Elsevier, 1991: pp. 9–28. doi:10.1016/b978-0-08-057116-4.50008-0.
32) A. Gandini, D. Coelho, M. Gomes, B. Reis, and A. Silvestre, "Materials from renewable resources based on furan monomers and furan chemistry: work in progress," J Mater Chem, 19 (45) 8656–8664 (2009). doi:10.1039/b909377j.
33) Fitri Ayu Radini, Dwi Novriadi, David N. Vicarneltor, Ara G. Rizkyta, Annisa Rifathin, Zarlina Zainuddin, Ade Pratama, Ade M. Wijaya, Reza Pahlevi Rudianto, and Riana Y.H. Sinaga, "Sustainable pallets from flexible multilayer plastic waste: a response surface and finite element analysis approach," Evergreen, 12 (1) 594–607 (2025). doi:10.5109/7342478.
34) E.R. Dyartanti, I.N. Widiasa, A. Purwanto, and H. Susanto, "Nanocomposite polymer electrolytes in pvdf/zno membranes modified with pvp for use in lifepo4 batteries," Evergreen, 5 (2) 19–25 (2018). doi:10.5109/1936213.
35) D. Ariawan, W.P. Raharjo, K. Diharjo, W.W. Raharjo, and B. Kusharjanta, "Influence of tropical climate exposure on the mechanical properties of rhdpe composites reinforced by zalacca midrib fibers," Evergreen, 9 (3) 662–672 (2022). doi:10.5109/4842526.
36) W. Wattanathana, Y. Hanlumyuang, S. Wannapaiboon, K. Chansaenpak, P. Pinyou, T. Nanok, and P. Kanjanaboos, "Novel dihydro-1,3,2h-benzoxazine derived from furfurylamine: crystal structure, hirshfeld surface analysis, photophysical property, and computational study," Crystals (Basel), 11 (5) (2021). doi:10.3390/cryst11050568.
37) D. Supramono, and J. Edgar, "Characteristics of non-polar bio-oil produced by co-pyrolysis of corn cobs and polypropylene using co2 as carrier gas," Evergreen, 6 (1) 78–84 (2019). doi:10.5109/2328407.
38) J. Wang, Q. Liu, J. Yu, R. Xu, C. Wang, and J. Xiong, "Synthesis and characterization of benzoxazine resin based on furfurylamine," Materials, 15 (23) (2022). doi:10.3390/ma15238364.
39) P. Madesh, S. Ramachandran, S. Appasamy, B. Krishnasamy, K. Muthu, and A. Muthukaruppan, "Valorization of agricultural waste to polybenzoxazine-carbon composites: studies on microstructure, thermal and dielectric properties," Eur Polym J, 197 (2023). doi:10.1016/j.eurpolymj.2023.112355.
40) E. Smith, and G. Dent, "Modern Raman

Spectroscopy-A Practical Approach," n.d.

41) K.S. Salem, N.K. Kasera, M.A. Rahman, H. Jameel, Y. Habibi, S.J. Eichhorn, A.D. French, L. Pal, and L.A. Lucia, "Comparison and assessment of methods for cellulose crystallinity determination," Chem Soc Rev, 52 (18) 6417–6446 (2023). doi:10.1039/d2cs00569g.
42) O.N. Tretinnikov, and S.A. Zagorskaya, "Determination of the degree of crystallinity of poly(vinyl alcohol) by ftir spectroscopy," J Appl Spectrosc, 79 (4) 521–526 (2012). doi:10.1007/s10812-012-9634-y.
43) M. Doumeng, L. Makhlouf, F. Berthet, O. Marsan, K. Delbé, J. Denape, and F. Chabert, "A comparative study of the crystallinity of polyetheretherketone by using density, dsc, xrd, and raman spectroscopy techniques," Polym Test, 93 (2021). doi:10.1016/j.polymertesting.2020.106878.
44) E. Tarani, I. Arvanitidis, D. Christofilos, D.N. Bikiaris, K. Chrissafis, and G. Vourlias, "Calculation of the degree of crystallinity of hdpe/gnps nanocomposites by using various experimental techniques: a comparative study," J Mater Sci, 58 (4) 1621–1639 (2023). doi:10.1007/s10853-022-08125-4.
45) C. Qian, Y. Zhao, Z. Wang, L. Liu, and D. Wang, "Probing the difference of crystalline modifications and structural disorder of isotactic polypropylene via high-resolution ftir spectroscopy," Polymer (Guildf), 224 (2021). doi:10.1016/j.polymer.2021.123722.